

AD-A281 959



S **DTIC**
ELECTE
JUL 21 1994
F

Chem. Phys. Lett. In press

July 1994

(1)

**EFFECT OF ION-ELECTRODE CONTACT ON THE ENERGETICS OF THE
HETEROGENEOUS ELECTRON TRANSFER.**

Xinfu Xia and Max L. Berkowitz

Department of Chemistry, University of North Carolina, Chapel Hill, NC 27599, USA

This document has been approved
for public release and sale; its
distribution is unlimited

Abstract: Using molecular dynamics computer simulation technique we studied the effect of the ion-electrode contact on the energetics of electron transfer reactions. We observed that when the solvation shell of the ion undergoes large changes due to the ion transfer from the bulk to the interface, the energetics of the reaction at the interface differs substantially from the energetics of the reaction in bulk.

94-22593



110

94 7 19

072

U.S. GOVERNMENT PRINTING OFFICE: 1989

Introduction.

Computer simulations play an important role in testing the validity of the ideas and assumptions made in theoretical description of the observed phenomena. For example, in the recent computer simulation for aqueous ferrous-ferric electron transfer it was observed that the Marcus relation [1,2] for intersecting parabolic diabatic free energy surfaces is quantitatively accurate [3].

While many electron transfer processes occur in the bulk phase, some of the important electron transfer processes occur at the interface. Therefore, it is very interesting to study how the energetics and dynamics of electron transfer process at the interface is different from the process that takes place in the bulk. Very recently two simulations performed by Straus and Voth [4] and by Rose and Benjamin [5] addressed this issue. Both simulations considered the electron transfer from the surface of Pt metal to the ion situated close to the surface. In both simulations the electron transfer occurred when the ion was situated ~ 0.5 nm away from the Pt surface, meaning that the ion in the simulations was still fully solvated by water, even while approaching the metal surface. This may correctly describe the situation for the Fe^{+3} ion, but it is not true for an ion such as I^- . Spohr [6] and Perera and Berkowitz [7] calculated the free energy profiles for the I^- ion solvated in water and approaching the Pt(100) surface, and obtained that most probable position of this ion at the interface is when it is in a contact with the surface of the metal. Because of the strong interaction between Li^+ ion and Pt metal surface, the calculation of the free energy profile for this ion shows that its most probable position is also in a contact with the surface [7]. That means that the solvation shells of Li^+ and I^- ions undergo a restructuring when these ions are transferred from the bulk to the interface. The influence of this restructuring on the energetics of the electron transfer process from and to the ions is studied in this paper.

Molecular Dynamics Simulations.

We consider here four molecular dynamics simulations, each performed in a box, which is $1.96 \times 1.96 \times 4.22$ nm³ in dimension and which contains 512 water molecules and one ion. Previous work shows that a system with these dimensions produces a correct water density in the center of the box. The system is periodical in x and y

dimensions and is restricted by Pt(100) surface in z dimension. It was also found [7] that I⁻ and Li⁺ ions, when adsorbed on the surface of the metal, are about 0.21 nm away from plane of the surface. The effect of the surface is completely diminished when the distance from the surface is above 1.0 nm. In each of the four simulations the ion is kept at the fixed position. In the first simulation (simulation A) the I⁻ ion is fixed at the interstitial position 0.21 nm away from Pt surface. In simulation B the Li⁺ ion is fixed at the same position. In the simulation C the I⁻ ion is fixed in the bulk water phase (1.61 nm away from the surface) and in simulation D a Li⁺ ion is fixed at the same distance from the surface.

The SPC/E model [8] was implemented to represent the water-water interaction. The ion-water interaction was represented by a Lennard-Jones plus Coulomb terms, i.e. we used the following form for this interaction:


$$U_{wi} = (A/r^{12} - C/r^6) + \sum_j q_i q_j / r_{ij} \quad (1)$$

In equation (1) r is the distance between the ion center and the oxygen site on the water, q_i the charge of the ion, q_j is the charge on the site j of water molecule, r_{ij} is the distance between the ion center and the site j of the water. The values of the parameters (A and C) for the ion-water Lennard-Jones interaction are

$A = 18927 \text{ \AA}^{12} \text{ kcal/mol}$, $C = 313.2 \text{ \AA}^6 \text{ kcal/mol}$ for the Li⁺ ion and

$A = 8993393 \text{ \AA}^{12} \text{ kcal/mol}$, $C = 2901.6 \text{ \AA}^6 \text{ kcal/mol}$ for the I⁻ ion (In reference 7, the parameters A and C for Li⁺-water interaction were reported as $A = 18927 \text{ \AA}^{12} \text{ kJ/mol}$, $C = 313.2 \text{ \AA}^6 \text{ kJ/mol}$, instead of $A = 18927 \text{ \AA}^{12} \text{ kcal/mol}$, $C = 313.2 \text{ \AA}^6 \text{ kcal/mol}$). To save a significant amount of computer time we represented the water-metal interaction in the same form as that used previously [9-11]. This form allowed us to concentrate on the motion of water molecules only, replacing all the Pt atoms by an effective field. The symmetry of the surface and its corrugation were also taken into account by the effective potential.

The equations of motion were solved using Verlet algorithm [12] and the water molecules were constrained to their geometries by implementing the Shake procedure [13]. The timestep used in all the simulations was 2.5 fs. We used a spherical cut-off scheme, with all interactions truncated at 0.98 nm (a smoothing of the potential over


Codes
Dist
A-1

the last 0.05 nm was applied). Corrections for the long range interactions were neglected beyond the cut-off distance. A temperature of ~300 K was maintained by the occasional rescaling of the velocities.

Free Energy Functions.

Free energy functions for the reactant and the product are defined as:

$$\Delta g_r(x) = -kT \ln P_r(x) \quad (2)$$

$$\Delta g_p(x) = -kT \ln P_p(x) + \Delta G_{pr} \quad (3)$$

where k is the Boltzmann constant, T is the temperature of the system and $P_r(x)$ and $P_p(x)$ are the probability distribution functions for the reactant and product respectively, x is a pre-defined reaction coordinate and ΔG_{pr} is the reaction free energy. It was demonstrated that [14,15]

$$\Delta g_p(x) = -x + \Delta g_r(x) \quad (4)$$

and therefore we only need to have one smooth curve of either $\Delta g_r(x)$ or $\Delta g_p(x)$ to obtain both curves. Following the well accepted convention [15], the reaction coordinate $\Delta\epsilon$ is defined as the difference in the solute-solvent interaction energy between the reactant and the product systems, i.e.

$$\Delta\epsilon = \epsilon_r - \epsilon_p \quad (5)$$

For any given configuration, this difference can be obtained in a straight forward manner by the following steps: first, calculate the interaction by setting the solute-solvent potential to that of the reactant; then, calculate the interaction by setting the potential function to that of the product; finally, calculate the difference in the interaction energies. In this work we assume that the Lennard-Jones part of the potential function is unchanged during the reaction. Hence the electrostatic energy due to the solute-solvent interaction represents the reaction coordinate. Having defined the reaction coordinate the probability distributions for the fluctuations and therefore free energy curves can be calculated as functions of this reaction coordinate. But the free energy curves can be reliably calculated only for x sufficiently close to the most probable value of the probability distribution $x = \langle \Delta\epsilon \rangle_r$, or $x = \langle \Delta\epsilon \rangle_p$. To obtain

a smooth free energy curve in the region far from $x = \langle \Delta\epsilon \rangle_r$, or $x = \langle \Delta\epsilon \rangle_p$, free energy perturbation and umbrella sampling techniques can be applied in the simulation [15]. A parameter α is therefore introduced to characterize the charging state of the solute, i.e.:

$$q_\alpha = (1-\alpha)q_r + \alpha q_p \quad (6)$$

The solute has the full charge of the reactant when $\alpha=0$, it has the charge of the product when $\alpha=1$. A molecular dynamics simulation is carried out with the certain value of the parameter α , ($0 < \alpha < 1$) and the free energy function is obtained from the expression

$$\Delta g_r^\alpha(x) = -kT \ln P_\alpha(x) + \alpha x + \Delta G_{\alpha 0} \quad (7)$$

Increasing α stepwise and repeatedly applying equation (7), the whole $\Delta g_r(x)$ can be constructed. In our calculations we performed at least 25 ps of molecular dynamics for each α to get a good convergence. To get a good precision in the evaluation of solute-solvent energy fluctuations at the minima of free energy curves, the simulations at these regions were performed for at least 100 ps. The curve for the $\Delta g_p(x)$ can be constructed with the help of equation (4). The free energy difference $\Delta G_{\alpha 0}$ that enters eq.(7) is obtained using the following equation

$$\Delta G_{\alpha 0} = -kT \ln [\langle \exp(-((H_\alpha - H_0)/kT)) \rangle_0] \quad (8)$$

which can also be calculated in a stepwise manner.

Results and Discussions.

We performed our calculations for the state when the Pt surface is at the potential of zero charge (pzc), therefore all the data for the free energy of the reaction, the transition free energy and reorganization free energy are given with respect to this state. The calculated free energy curves $\Delta g_r(x)$ (the curves on the left) and $\Delta g_p(x)$ (the curves on the right) are shown in Figure 1a (for I at the interface), Figure 1b (for I in bulk), Figure 2a (for Li^+ at the interface) and Figure 2b (for Li^+ in bulk). In Figures 1a and 1b the curves on the left are for the iodide ion in its charged state, so that the reaction corresponds to the process of oxidation of the ion. From the comparison of

these two figures we observe that the partial removal of solvation water results in a smaller free energy of the oxidation reaction, as expected. The calculations show that when the iodide is on the surface $\Delta G_{pr} = 153$ kJ/mol and the reorganization energy is 195 kJ/mol, while when the iodide is in the bulk $\Delta G_{pr} = 237$ kJ/mol and the reorganization energy is 280 kJ/mol. The relatively large change in the energetics of the electron transfer reaction observed in the case of I⁻ ion (the reaction free energy is changed by 55%, while the reorganization energy is changed by 44%) is due to the large change in the solvation shell around the ion, when it is transferred from the bulk to the surface. As it was observed previously [7] the coordination number of I⁻ changes from ~7 to ~4 during this transfer.

What about the energetics of the reaction $\text{Li}(\text{aq}) \rightarrow \text{Li}^+(\text{aq}) + e^-$? The free energy curves for this process are depicted in Figures 2a and 2b, where the left curves correspond to the uncharged state of the ion, so that the reaction again corresponds to the oxidation process. The calculations show that in case of the lithium ion the free energy of the reaction and reorganization free energy are nearly the same when the reaction takes place at the surface or in the bulk. Thus for the reaction on the surface $\Delta G_{pr} = -512$ kJ/mol, while for the reaction in bulk $\Delta G_{pr} = -548$ kJ/mol (the change is only 7%). The absolute value of the change of reorganization free energy is rather large (reorganization free energy on the surface is 346 kJ/mol, in bulk it is equal to 445 kJ/mol), but the relative value of the change (29%) is still smaller than for I⁻ case (44%). The smaller change in the energetics of this reaction compared to the reaction with iodide is explained by the fact that the solvation of the Li⁺ ion is not changed dramatically, when the ion is moved from the bulk phase to the surface. Thus Perera and Berkowitz find that although the first solvation shell of water is restructured around the ion, the coordination number remains the same (~4) [7].

An issue often discussed in the literature is how good is the quadratic approximation to the free energy curves. If the true free energy curve is quadratic, then the curve has a constant curvature that can be obtained from the bottom region of the curve. The free energy curves with the curvatures obtained from such fit ("bottom" curvatures) are represented in the Figures 1 and 2 by thin lines. As we can see these curves approximate reasonably well the free energy curves for I⁻ obtained from the simulations. We also observe that the "bottom" curvatures of the reactant

curves is smaller than the "bottom" curvatures of the product curves, i.e. that the solute-solvent energy fluctuations which determine the magnitude of the curvature at the bottom of free energy curves are larger when the dynamics is performed with the charged state of the ion. This is contrary to the behavior observed in the previous simulations [5]. But in the previous simulations the ion was positively charged, while in the present simulation the iodide ion is negatively charged. If the ion is negatively charged, the neighbouring water molecule places its hydrogen closest to the ion. When the dynamics is performed on the product surface the ion is neutral and therefore the water hydrogens are further away from the ion. Due to the proximity of the hydrogens to the charged ion the amplitude of the fluctuations in ion-water energy is larger when the dynamics is performed in the charged ion state.

As Figures 2a and 2b show the quadratic curves (with curvatures obtained by a fit to the bottom of the true free energies) do not approximate well the curves from the calculations. Also the "bottom" curvatures for the reactant curve and the product curves are different, and again the "bottom" curvature of the reactant curve is smaller than the "bottom" curvature of the product curve. But this time the reactant curve is obtained from the dynamics with the uncharged ion, while the dynamics with the charged ion is used to get the product curve. This time the hydrogen atoms of water are closest to ions when the dynamics is done with the ion in its uncharged state. We observe that the ion-water energy fluctuations now have the same character as in the previous simulations [4,5], which were also performed for the positively charged ions.

As was pointed out by Tachiya [14], when the "bottom" curvatures of free energy curves are different, the condition imposed by eq. (4) is violated. To satisfy this condition we can fit one of the free energy curves (for reactant or product) and obtain the second free energy curve from the application of eq. (4), similarly to the procedure performed by Straus and Voth [4]. The curves obtained in this way are also shown (broken lines) in Figures 1 and 2. In all cases we obtained the broken curves by performing the best fit to the upper free energy curve, while the lower curve was obtained from the upper by using equation (4). As we can see from Figures 1 and 2 this fit with the "global" curvature shows that although we do observe deviations from quadratic behavior of free energies, nevertheless large regions of free energy curves do look parabolic. And this is correct for both anion and cation. According to Marcus

for any intersecting parabolic free energy curves of equal curvature there is a universal relationship between the activation free energy (ΔG^*) and the reaction free energy (ΔG^0), which has the form:

$$\Delta G^* = (\Delta G^0 + \lambda)^2 / 4\lambda \quad (9)$$

In eq. (9) λ is the reorganization free energy. The test of equation (9) for calculated free energies is shown in Figure 3. As we can see the calculations display deviations from Marcus curve, mostly in the inverted region. The closest to Marcus curve behavior is observed for the reaction $I(aq) \rightarrow I(aq) + e$ in bulk, while the largest deviation from Marcus curve is observed for the reaction $Li(aq) \rightarrow Li^+(aq) + e$ at the interface.

Figures 4 and 5 show how the reaction activation free energy depends on the overvoltage. We follow the standard convention and assume that the overvoltage η is zero when the reaction free energy ΔG_{pr} is zero. Figure 4 presents plots for the oxidation reaction for I ion when it occurs on the surface and in bulk. As we can see from this figure the reaction energetics on the surface and in bulk is substantially different. Figure 5 presents same type of plots for the oxidation reaction for Li. This time we do not see a large change in the energetics of the reaction in agreement with what was already mentioned above.

Finally we want to mention here that the present calculations should be considered as model calculations rather than quantitative, since the quantitative values will depend strongly on the potentials used in the simulations and on the treatment of long range forces and the treatment of water and ion polarization. In this paper we used the same ion-surface interaction potential as the one presented by Seitz-Beywl et. al. in reference [16], where they investigated the structure and dynamics of LiF aqueous solution next to Pt(100) surface. The same potential was later used by Spohr [6] and by Perera and Berkowitz [7] to get the potentials of mean force for I approaching Pt(100) and Li^+ approaching Pt(100) surface. This ion-surface potential neglects to consider that partial charge transfer between the hydrated ion and platinum surface may occur. According to estimates performed recently by Nazmutdinov and Spohr [17], partial charge transfer can be rather substantial in the case of I ion. The ion-surface potential that we use also neglects the surface

polarization due to the ion. The polarization of the surface due to the charges is often treated using image charge method, but this method fails to describe appropriately the interaction of water molecules close to the interface with the surface of a metal such as Pt [18]. To consider the effect of surface polarization due to the ion on the dynamics of water one can use a mixed approach, where the image charge method is used to describe ion/metal interaction, while potentials like the one described in reference [9] are used to describe water/metal interaction. Unfortunately, it is not known if such an approach is correct. More studies to test this approach and to investigate the effect of surface polarizability on the energetics and kinetics of electron transfer at the interface are needed. Surface polarizability may play an important role in the electron transfer energetics, but we believe that the major change in the energetics (when such a change exists) is due to the large restructuring of the first solvation shell when the ion is adsorbed on the surface, like in the case observed for the I⁻ ion in the present simulations.

Acknowledgment: This research was supported by the Office of Naval Research. We are grateful to the referee for careful reading of the manuscript and for useful suggestions.

References and Notes

- [1] Marcus, R.A. *Ann. Rev. Phys. Chem.* 1964, 15, 155.
- [2] Marcus, R.A.; Sutin, N. *Biochim. Biophys. Acta* 1985, 811, 265.
- [3] Kuharski, R.A.; Bader, J. S.; Chandler, D.; Sprik, M.; Klein, M.L.; Impey, R.W. *J. Chem. Phys.* 1988, 89, 3248
- [4] Straus, J. B.; Voth, G.A. *J. Phys. Chem.* 1993, 97, 7388
- [5] Rose, D; Benjamin, I. *J. Chem. Phys.* 1994, 100, 3545
- [6] Spohr, E. *Chem. Phys. Lett.* 1993, 207, 214
- [7] Perera, L.; Berkowitz, M. *J. Phys. Chem.* 1993, 97, 13803
- [8] Berendsen, H.J.C.; Grigera, J.R.; and Straatsma, T.P. *J. Phys. Chem.* 1987, 91, 6269
- [9] Foster, K.; Raghavan, K; and Berkowitz, M. *Chem. Phys. Lett.* 1989, 32, 162
- [10] Raghavan, K.; Foster, K.; Motakabbir, K.; and Berkowitz, M. *J. Chem. Phys.* 1991, 2110, 94
- [11] Raghavan, K.; Foster, K.; and Berkowitz, M. *Chem. Phys. Lett.* 1991, 177, 426
- [12] Verlet, L. *Phys. Rev.* 1967, 98, 159
- [13] Ryckaert, J.P.; Ciccotti, G.; and Berendsen, H.J.C. *J. Comput. Phys.* 1977, 23, 327
- [14] Tachiya, M. *J. Phys. Chem.* 1989, 93, 7050
- [15] King, J.; Warshel A. *J. Chem. Phys.* 1990, 93, 8682
- [16] Seitz-Beywl, J; Poxleitner, M.; Heinzinger, K. *Z. Naturforsch.* 1991, 46A, 876
- [17] Nazmutdinov, R.R.; Spohr, E. *J. Phys. Chem.* 1994, 98, 5956
- [18] Spohr, E.; Heinzinger, K. *Ber. Bunsenges. Phys. Chem.* 1988, 92, 1358

Figure 1. Free energy curves for the reaction, $I^- \rightarrow I + e$, (a) at the platinum-water interface; (b) in the bulk water. The reactant curves, $\Delta g_r(x)$, are on the left. The product curves, $\Delta g_p(x)$, are on the right. The thick solid lines are obtained from the MD simulations by using Equation (2), (3), and (7). The dashed lines are parabolic curves, $k(x - b)^2 + c$, fit to the thick solid lines. The parameters are $k = 1.32 \times 10^{-3}$ mol/kJ, $b = 46$ kJ/mol, and $c = 154$ kJ/mol for the reaction at the interface; and $k = 1.00 \times 10^{-3}$ mol/kJ, $b = 43$ kJ/mol, and $c = 237$ kJ/mol for the bulk reaction. The thin solid lines are parabolic curves with the curvature obtained from the fit to the bottom of the thick solid curves.

Figure 2. Free energy curves for the reaction, $Li \rightarrow Li^+ + e$, (a) at the platinum-water interface; (b) in the bulk water. Symbols have the same meanings as in Figure 1. The parameters are: $k = 3.00 \times 10^{-4}$ mol/kJ, $b = 6.12$ kJ/mol, $c = 512$ kJ/mol for the reaction at the interface; and $k = 4.66 \times 10^{-4}$ mol/kJ, $b = 27.5$ kJ/mol, and $c = 548.0$ kJ/mol for the reaction in the bulk.

Figure 3. The relationship between the activation free energy $-\Delta G^*/\lambda$ and the reaction free energy $-\Delta G^0/\lambda$. The Marcus relationship (thick line) is also plotted for comparison.

Figure 4. Activation free energy vs. the overvoltage η for the reaction, $I^- \rightarrow I + e$, in the bulk water (solid line) and at the Pt-water interface (dashed line).

Figure 5. Activation free energy vs. the overvoltage η for the reaction, $Li \rightarrow Li^+ + e$, in the bulk water (solid line) and at the Pt-water interface (dashed line).

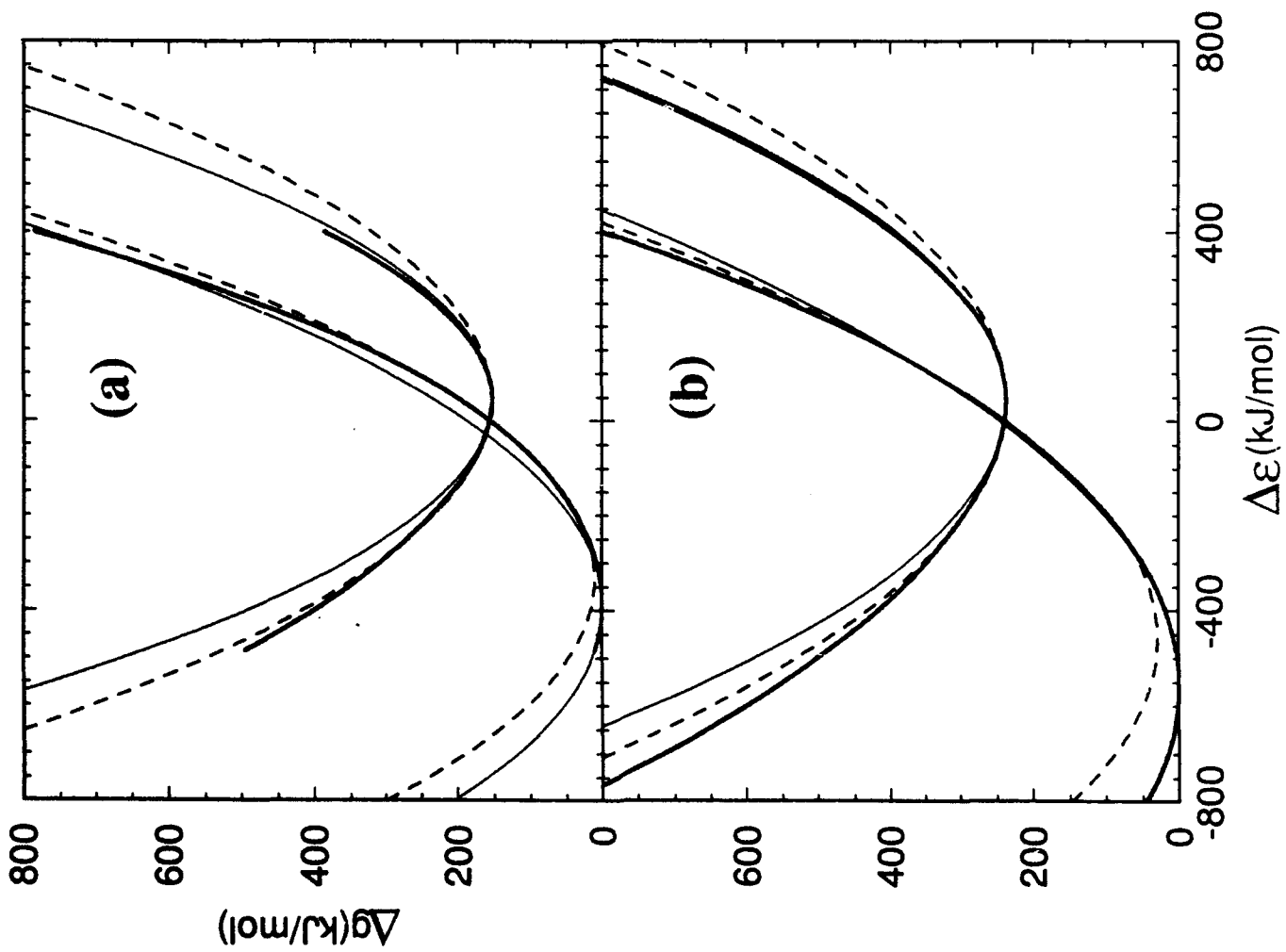


Fig. 1

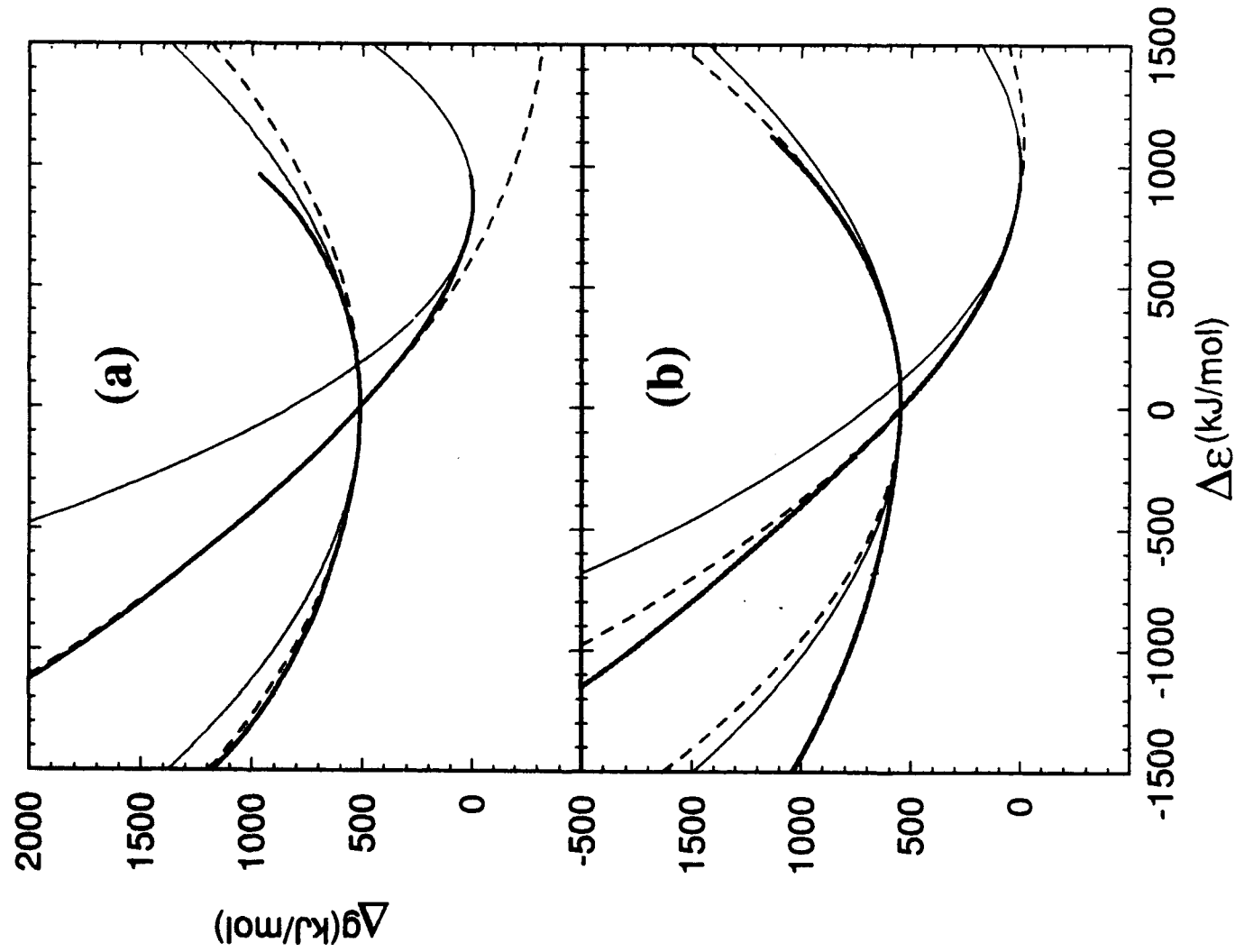


Fig. 2

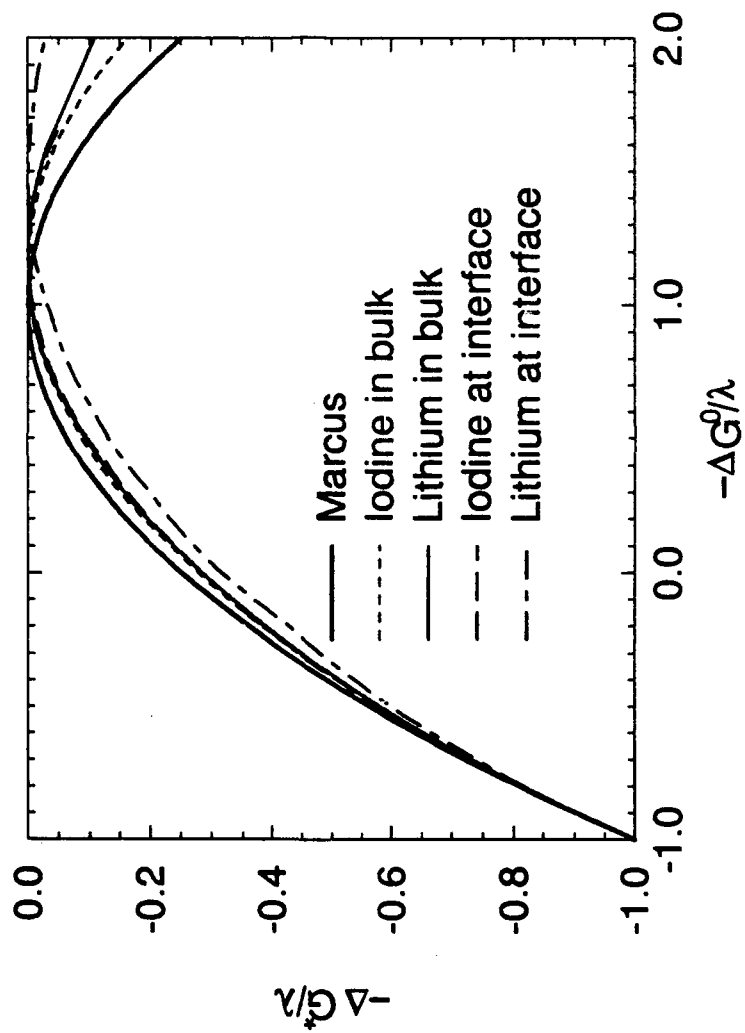


Fig. 3

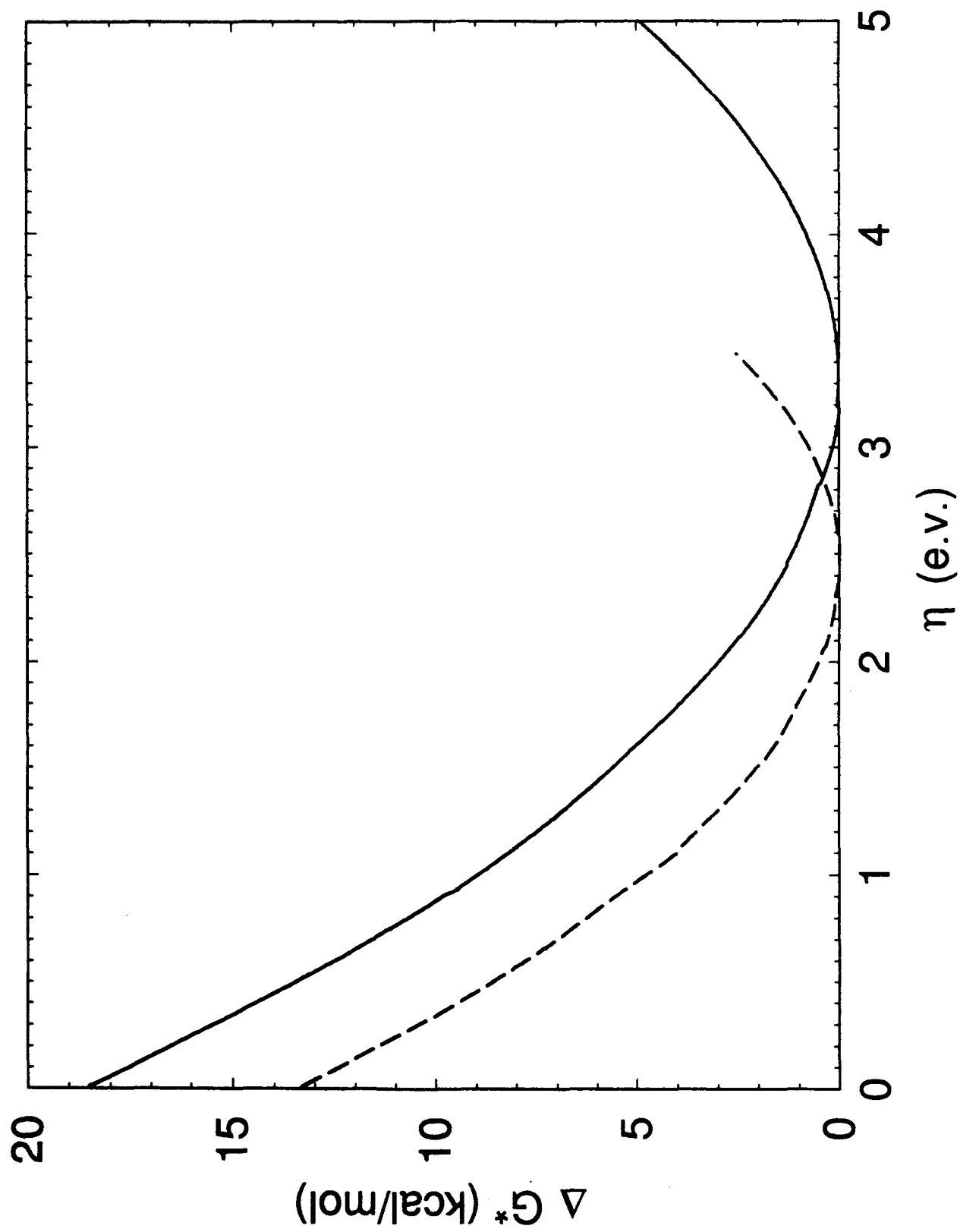


Fig. 4

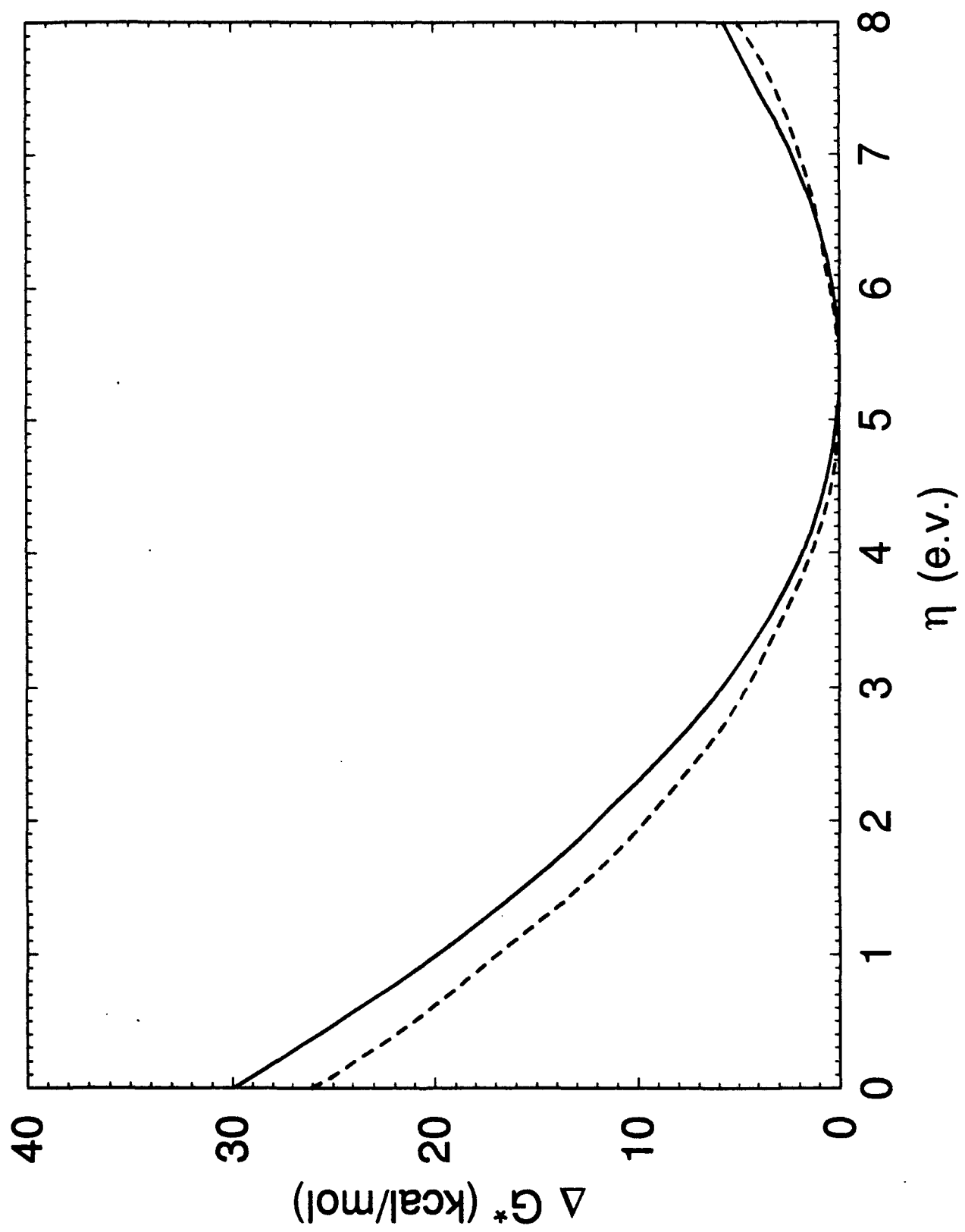


Fig. 5.